

The $b \rightarrow X_s \gamma$ rate and Higgs boson limits in the Constrained Minimal Supersymmetric Model

W. de Boer, M. Huber

*Institut für Experimentelle Kernphysik, University of Karlsruhe
Postfach 6980, D-76128 Karlsruhe, Germany*

A.V. Gladyshev, D.I. Kazakov

*Bogoliubov Laboratory of Theoretical Physics, Joint Institute for Nuclear Research,
141 980 Dubna, Moscow Region, Russian Federation*

Abstract

New NLO $b \rightarrow X_s \gamma$ calculations have become available using resummed radiative corrections. Using these calculations we perform a global fit of the supergravity inspired constrained minimal supersymmetric model. We find that the resummed calculations show similar constraints as the LO calculations, namely that only with a relatively heavy supersymmetric mass spectrum of $\mathcal{O}(1 \text{ TeV})$ the $b-\tau$ Yukawa unification and the $b \rightarrow X_s \gamma$ rate can coexist in the large $\tan \beta$ scenario. The resummed $b \rightarrow X_s \gamma$ calculations are found to reduce the renormalization scale uncertainty considerably. The low $\tan \beta$ scenario is excluded by the present Higgs limits from LEP II. The constraint from the Higgs limit in the $m_0, m_{1/2}$ plane is severe, if the trilinear coupling A_0 at the GUT scale is fixed to zero, but is considerably reduced for $A_0 \leq -2m_0$. The relatively heavy SUSY spectrum required by $b \rightarrow X_s \gamma$ corresponds to a Higgs mass of $m_h = 119 \pm 1$ (stop masses) ± 2 (*theory*) ± 3 (top mass) GeV in the CMSSM.

1 Introduction

In a previous paper we showed that the inclusive decay rate $b \rightarrow X_s \gamma$ at leading order (LO) severely constrains the high $\tan \beta$ solution of the Constrained Minimal Supersymmetric Standard Model (CMSSM) [1]. This was mainly caused by the fact that $b-\tau$ Yukawa coupling unification preferred a negative sign for the Higgs mixing parameter μ , while the $b \rightarrow X_s \gamma$ rate required the opposite sign. With initial next-to-leading order (NLO) calculations for the $b \rightarrow X_s \gamma$ rate in the MSSM [2] large terms proportional to $\tan^2 \beta$ changed the sign of μ [3]. However, some sign errors in Ref. [2] were detected [4, 5] and with the corrected sign we found that no change of the sign of the chargino-stop amplitude occurred anymore, although the NLO corrections were still large. Resumming of the large terms was done in Refs. [4, 5] and especially the contributions from the heavier stop, which were neglected in Ref. [2], were taken into account. Due to a large cancellation between the stop1

and stop2 contributions, the NLO corrections turn out to be relatively small, so similar results as in LO can be expected.

In our statistical χ^2 analysis the constraints from gauge coupling unification, $b - \tau$ Yukawa coupling unification, electroweak symmetry breaking, $b \rightarrow X_s \gamma$, relic density and experimental lower limits on SUSY masses can be considered either separately or combined[1]. Constraints from LO $b \rightarrow X_s \gamma$ rates were considered before in Refs. [6]. As input parameters of the Constrained MSSM (CMSSM) we consider at the unification scale (M_{GUT}) the unified gauge coupling constant (α_{GUT}), the Yukawa coupling constants of the third generation (Y_t^0, Y_b^0, Y_τ^0), the common scalar mass (m_0), the common gaugino mass ($m_{1/2}$), the common trilinear coupling ($A_t^0 = A_b^0 = A_\tau^0$), and the Higgs mixing parameter μ^0 . Furthermore the ratio of the vacuum expectation values of the two Higgs doublets ($\tan \beta$) is a free parameter. These parameters are optimized via a χ^2 test to fit the low energy experimental data on electroweak boson masses, $b \rightarrow X_s \gamma$, and quark and lepton masses of the third generation. Details can be found in Refs. [1, 7].

The values of m_0 , $m_{1/2}$, μ^0 , A^0 , Y^0 and $\tan \beta$ determine completely the mass spectrum of all SUSY particles via the RGE. The values of μ^0 , Y^0 and $\tan \beta$ are constrained for given values of m_0 and $m_{1/2}$ by EWSB and the quark and lepton masses of the third generation. Since m_0 and $m_{1/2}$ are strongly correlated, we repeat each fit for every pair of m_0 and $m_{1/2}$ values between (200,200) and (1000,1000) GeV in steps of 100 GeV.

The present value of the top mass of 174.3 ± 5.1 [8] constrains $\tan \beta$ to the regions 1.6 ± 0.3 and 35 ± 3 (see Fig. 1), which we call the low and high $\tan \beta$ scenario, respectively. The high $\tan \beta$ scenario requires $\mu < 0$, since the χ^2 minimum of 19 for $\mu > 0$ at $\tan \beta \approx 60$ is excluded now by the top mass value.

At $\tan \beta = 35$ the top and bottom-tau Yukawa couplings are of the same order of magnitude. Forcing triple Yukawa unification would increase $\tan \beta$ somewhat (see middle part of Fig. 1). EWSB would then require a slight splitting in the mass parameters of the two Higgs doublets, which is possible by non-universal terms at the GUT scale[9]. However, the whole picture and mass spectra would not change significantly.

In the next section we consider NLO corrections to $b \rightarrow X_s \gamma$ in order to check whether they are consistent with the $\mu < 0$ solution at $\tan \beta = 35$, since the solution at $\tan \beta = 1.65$ is excluded by the present Higgs limit of 113.5 GeV[10], as will be discussed in the last section.

2 NLO corrections to $b \rightarrow X_s \gamma$

We use the $b \rightarrow X_s \gamma$ rate from the CLEO Collaboration [11]: $BR(b \rightarrow X_s \gamma) = (3.15 \pm 0.35 \pm 0.32 \pm 0.26) \cdot 10^{-4}$. This value combined with the less precise ALEPH measurement [12] of $BR(b \rightarrow X_s \gamma) = (3.11 \pm 0.80 \pm 0.72) \cdot 10^{-4}$ yields as average $BR(b \rightarrow X_s \gamma) = (3.14 \pm 0.48) \cdot 10^{-4}$.

The $b \rightarrow X_s \gamma$ transition corresponds in lowest order to a loop with either a W, charged Higgs or chargino. The leading order corresponds to the emission of a real photon from any of the charged lines, while the dominant next-to-leading

order (NLO) corrections involve virtual gluons from any of the (s)quark lines. The theoretical calculations of the $b \rightarrow X_s \gamma$ rate are well advanced. The LO Standard Model (SM) calculations [13, 14, 15] have been complemented by NLO calculations [16, 17, 18, 19]. Recently, NLO calculations have been extended to Two-Higgs Doublet Models (2HDM) [20, 21] and the Minimal Supersymmetric Model (MSSM) [2, 4, 5, 22]. Here we use the results from Ref. [5], which include all potentially large two-loop contributions.

Fig. 2 shows the value of $b \rightarrow X_s \gamma$ decay rate as function of $\tan \beta$ for two choices of the universal masses at the GUT scale, namely $m_0 = 600$, $m_{1/2} = 400$ and $m_0 = 1000$, $m_{1/2} = 1000$ GeV. In order to get good agreement with the data at large $\tan \beta$ one needs heavy sparticles, as shown by the plots at the bottom. The renormalization scale dependence in NLO is considerably reduced as compared to the LO calculations, as shown by the width of the bands in Fig. 2. Here we only considered the dominant scale uncertainty from the low energy scale, which was varied between $0.5m_b$ and $2m_b$. The effect of the NLO calculations including both stops and resummed corrections on the total rate and individual amplitudes is rather small, as can be seen from the comparison of the LO and NLO rate and amplitudes shown in Fig. 3. So, the results at large $\tan \beta$ are similar to the previous LO calculations[1], but slightly more restrictive due to the smaller scale uncertainty in the NLO.

Fig. 4 shows the χ^2 distribution in the $m_0, m_{1/2}$ plane with the dominant source of the excluded regions in the contours at the bottom. The analysis from Ref. [23] finds a more restricted region, mainly because they require the relic density to be between 0.1 and 0.3, while we require simply that the relic density is not above the critical density. The low $\tan \beta$ scenario from Ref. [1] is shown for comparison. Previously it was constrained mostly by the relic density, although now the whole low $\tan \beta$ scenario is excluded by the present limits on the Higgs mass from LEP, as will be discussed in the next section.

3 Higgs mass constraints

In Supersymmetry the couplings in the Higgs potential are the gauge couplings. The absence of arbitrary couplings together with well defined radiative corrections to the masses results in clear predictions for the lightest Higgs mass and electroweak symmetry breaking (EWSB)[24].

In the Born approximation one expects the lightest Higgs to have a mass m_h below the Z^0 mass. However, loop corrections, especially from top and stop quarks, can increase m_h considerably[25]. The Higgs mass depends mainly on the following parameters: the top mass, the squark masses, the mixing in the stop sector, the pseudoscalar Higgs mass and $\tan \beta$. As will be shown below, the maximum Higgs mass is obtained for large $\tan \beta$, for a maximum value of the top and squark masses and a minimum value of the stop mixing. The Higgs mass calculations were carried out following the results obtained by Carena, Quirós and Wagner[26] in a renormalization group improved effective potential approach, including the dominant two-loop contributions from gluons and gluinos. The gluino contributions were

taken from the FeynHiggs calculations[27].

Note that in the CMSSM the Higgs mixing parameter μ is determined by the requirement of EWSB, which yields large values for μ [24]. Given that the pseudoscalar Higgs mass increases rapidly with μ , this mass is always much larger than the lightest Higgs mass and thus decouples. We found that this decoupling is effective for all regions of the CMSSM parameter space, i.e. the lightest Higgs has the couplings of the SM Higgs within a few percent. Consequently, the experimental limits on the SM Higgs can be taken.

The lightest Higgs boson mass m_h is shown as function of $\tan\beta$ in Fig. 5. The shaded band corresponds to the uncertainty from the stop mass for $m_t = 175$ GeV. The upper and lower lines correspond to $m_t=170$ and 180 GeV, respectively.

One observes that for a SM Higgs limit of 113.5 GeV [10] all values of $\tan\beta$ below 4.3 are excluded in the CMSSM. This implies that the low $\tan\beta$ scenario with $\tan\beta = 1.6 \pm 0.3$ (see Fig. 1) is excluded.

In order to estimate the uncertainties of the Higgs mass predictions in the CMSSM, the relevant parameters were varied one by one. The Higgs mass varies between 110 and 120 GeV, if m_0 and $m_{1/2}$ are varied between 200 and 1000 GeV, which implies stop masses varying between 400 and 2000 GeV, as shown in Fig. 6 for three different values of the trilinear coupling at the GUT scale A_0 in units of m_0 . For larger values of $m_{1/2}$ and $\tan\beta$ the Higgs mass saturates, as is obvious from the 3-D plots in Fig. 6 and from Fig. 5. The $b \rightarrow X_s \gamma$ rate requires $A_0 > -2m_0$, since lower values increase $b \rightarrow X_s \gamma$ even more for $\mu < 0$. For $A_0 = -2m_0$ $m_h > 113.5$ GeV excludes only the small corner at the left bottom in the $m_0, m_{1/2}$ plane. In Ref. [23] the excluded region is larger, since they kept $A_0 = 0$. Note that the stop mixing parameter $X_t = A_t - \mu/\tan\beta$ is not an arbitrary free parameter in the CMSSM, since the Higgs mixing parameter μ is determined by EWSB and the value of A_t at low energy is largely determined by $m_{1/2}$ through radiative corrections, so the Higgs mass uncertainty from the stop mixing is included in the variation of m_0 and $m_{1/2}$. One observes from Fig. 5 that at large $\tan\beta$ the Higgs mass varies between 110 and 120 GeV, if the SUSY mass parameters are varied up to 1 TeV. We take the variance of this interval, which is $10/\sqrt{12}=3$ GeV, as an error estimate for the uncertainty from the stop masses. The values $m_0 = m_{1/2} = 370$ GeV yield the central value of $m_h = 115$ GeV.

The dependence on m_t is shown in Fig. 7 for $A_0 = 0$ and intermediate values of m_0 and $m_{1/2}$ for two values of $\tan\beta$ (corresponding to the minimum χ^2 values in Fig. 1). The uncertainty from the top mass at large $\tan\beta$ is ± 5 GeV, given the uncertainty on the top mass of 5.2 GeV. The uncertainty from the higher order calculations (HO) is estimated to be 2 GeV from a comparison of the full diagrammatic method [27] and the effective potential approach[26], so combining all the uncertainties discussed before we find for the Higgs mass in the CMSSM

$$m_h = 115 \pm 3 \text{ (stop masses)} \pm 2 \text{ (theory)} \pm 5 \text{ (top mass)} \text{ GeV}, \quad (1)$$

where the errors are the estimated standard deviations around the central value. As can be seen from Fig. 5 this central value is valid for all $\tan\beta > 20$ and decreases for lower $\tan\beta$.

If we include previous constraints from $b \rightarrow X_s \gamma$, than the allowed region is restricted by $m_{1/2} > 700$ GeV, leading to heavy stop masses. This results in a heavier Higgs mass with a reduced error due to the saturation of the Higgs mass for large sparticle masses:

$$m_h = 119 \pm 1 \text{ (stop masses)} \pm 2 \text{ (theory)} \pm 3 \text{ (top mass)} \text{ GeV.} \quad (2)$$

4 Conclusions

The results can be summarized as follows:

- The NLO $b \rightarrow X_s \gamma$ contributions do not strongly change the LO predictions; only the renormalization scale uncertainty decreases, thus increasing the excluded parameter region. The observed $b \rightarrow X_s \gamma$ is still difficult to reconcile at large $\tan \beta$ with $b - \tau$ unification, as observed before in LO[1].
- The low $\tan \beta$ scenario ($\tan \beta < 4.3$) of the CMSSM is excluded by the 95 % C.L. lower limit on the Higgs mass of 113.5 GeV[10].
- For the high $\tan \beta$ scenario the Higgs mass is found to be below 125 GeV in the CMSSM. This prediction is independent of $\tan \beta$ for $\tan \beta > 20$ and decreases for lower $\tan \beta$. The Higgs mass corresponding to the relatively heavy sparticle spectrum required by the $b \rightarrow X_s \gamma$ measurement is: $m_h = 119 \pm 1 \text{ (stop masses)} \pm 2 \text{ (theory)} \pm 3 \text{ (top mass)} \text{ GeV}$.
- The constraint in the $m_0, m_{1/2}$ plane by the present Higgs limit of 113.5 GeV is severe, if the trilinear coupling A_0 is chosen to be positive at the GUT scale, but is strongly reduced for $A_0 \leq -2m_0$.

Acknowledgements

A.G. and D.K. would like to thank the Heisenberg-Landau Programme and RFBR grant # 99-02-16650 for financial support and the Karlsruhe University for hospitality during the time this work was carried out.

Note added in proof.

Recently the Muon (g-2) Collaboration (H.N. Brown et al., hep-ex/0102017) has measured the anomalous magnetic moment of the muon. They find a 2.6σ deviation from the SM expectation. If interpreted as contributions from supersymmetry, then this measurement would require $\mu > 0$ in our conventions. This would be opposite to the sign required by $b - \tau$ unification, so to include this measurement would require to give up $b - \tau$ unification or to modify the CMSSM, e.g. by including complex phases. This will be studied in a forthcoming paper.

References

- [1] W. de Boer, H.-J. Grimm, A.V. Gladyshev, D.I. Kazakov, Phys. Lett. **B 438** (1998) 281.
- [2] M. Ciuchini, G. Degrassi, P. Gambino, G.F. Giudice, Nucl. Phys. **B 534** (1998) 3-20.
- [3] W. de Boer, M. Huber, A. Gladyshev and D. I. Kazakov, hep-ph/0007078, contributed paper to ICHEP 2000, Osaka, Aug. 2000.
- [4] M. Carena, D. Garcia, U. Nierste and C. E. Wagner, hep-ph/0010003.
- [5] G. Degrassi, P. Gambino and G. F. Giudice, JHEP**0012** (2000) 009.
- [6] R. Barbieri and G.F. Giudice, Phys. Lett. **B309** (1993) 86;
R. Garisto and J. Ng, Phys. Lett. **B315** (1993) 372;
F. Borzumati, Z.Phys. **C63** (1994) 291;
F. Borzumati, M. Olechowski and S. Pokorski, Phys. Lett. **B349** (1995) 311;
J.L. Hewett and J.D. Wells, Phys. Rev. **D55** (1997) 5549,
T. Blazek, M. Carena, S. Raby and C.E.M. Wagner, Phys.Rev. **D56** (1997) 6919;
T. Blazek and S. Raby, Phys. Rev. **D59** (1999) 95002.
- [7] W. de Boer, et al. Z.Phys. **C67** (1995) 647; *ibid* **C71** (1996) 415.
- [8] Particle Data book, Eur. Phys. J. **C3** (1998) 1.
- [9] N. Polonsky, A. Pomarol, Phys.Rev.Lett. 73 (1994) 2292; Phys.Rev. D51 (1995) 653
- [10] ALEPH Coll., R. Barate et al., Phys. Lett. **B495** (2000) 1;
L3 Coll., M. Acciarri et al., Phys. Lett. **B495** (2000) 18;
DELPHI Coll., P. Abreu et al., Phys. Lett. **B499** (2001) 23;
OPAL Coll., G. Abbiendi et al., Phys. Lett. **B499** (2001) 38;
The combined results were given by P. Igo-Kemenes, LEP Seminar, Nov. 3, CERN, <http://lephiggs.web.cern.ch/LEPHIGGS/talks/index.html>.
Although the data is consistent with a Higgs of 115 GeV, the deviation from the SM is of the order of 3 standard deviations and to be considered preliminary..
Therefore we only consider the lower limit of 113.5 GeV at present.
- [11] CLEO Coll., S. Ahmed et al., CLEO CONF 99/10, hep-ex/9908022.
- [12] R. Barate et al. (ALEPH Collaboration), Phys. Lett. **B 429** (1998) 169.
- [13] B. Grinstein, R. Springer and M.B. Wise, Nucl. Phys. **B 339**, 269 (1990).
- [14] S. Bertolini, F. Borzumati, A. Masiero, G. Ridolfi, Nucl. Phys. **B 353** (1991) 591,
V. Barger, M.S. Berger, P. Ohmann and R.J.N. Phillips, Phys. Rev. **D51** (1995) 2438,
H. Baer and M. Brhlik, Phys. Rev. **D55** (1997) 3201.
- [15] A.J. Buras, M. Misiak, M. Münz and S. Pokorski, Nucl. Phys. **B 424**, 374 (1994).

- [16] K. Adel and Y.P. Yao, Phys. Rev. **D 49**, 4945 (1994).
- [17] C. Greub and T. Hurth, Phys. Rev. **D 56**, 2934 (1997).
- [18] A. Ali and C. Greub, Phys. Lett. **B 361**, 146 (1995). A. Ali, C. Greub, Z.Phys. **C 60** (1993) 433.
- [19] C. Greub, T. Hurth and D. Wyler, Phys.Lett. **B 380**, 385 (1996); Phys. Rev. **D 54**, 3350 (1996).
- [20] M. Ciuchini, G. Degrassi, P. Gambino and G.F. Giudice, Nucl. Phys. **B 527** (1998) 21-43.
- [21] F.M. Borzumati and C. Greub, Phys. Rev. **D58** (1999) 074004; *ibid* **D59** (1999) 057501.
- [22] C. Bobeth, M. Misiak, and J. Urban, TUM-HEP-321-98, hep-ph/9904413, Nucl. Phys. **B 567** (2000) 153.
- [23] J. Ellis, G. Ganis, D.V. Nanopoulos, K. Olive, hep-ph/0009355, Phys. Lett. **B502** (2001) 171.
- [24] See e.g. W. de Boer, Prog. Part. Nucl. Phys. **33**(1994) 201 and references therein.
- [25] J. Ellis, G. Ridolfi, F. Zwirner, Phys.Lett. **B262** (1991) 477
- [26] M. Carena, M. Quirós and C. Wagner, Nucl. Phys. **B 461** (1996) 407
- [27] M. Carena et al., Nucl. Phys. **B580** (2000) 29; S. Heinmeyer, W. Hollik, G. Weiglein, Phys. Lett. **B455** (1999) 179; Euro. Phys. J. **C9** (1999) 343.

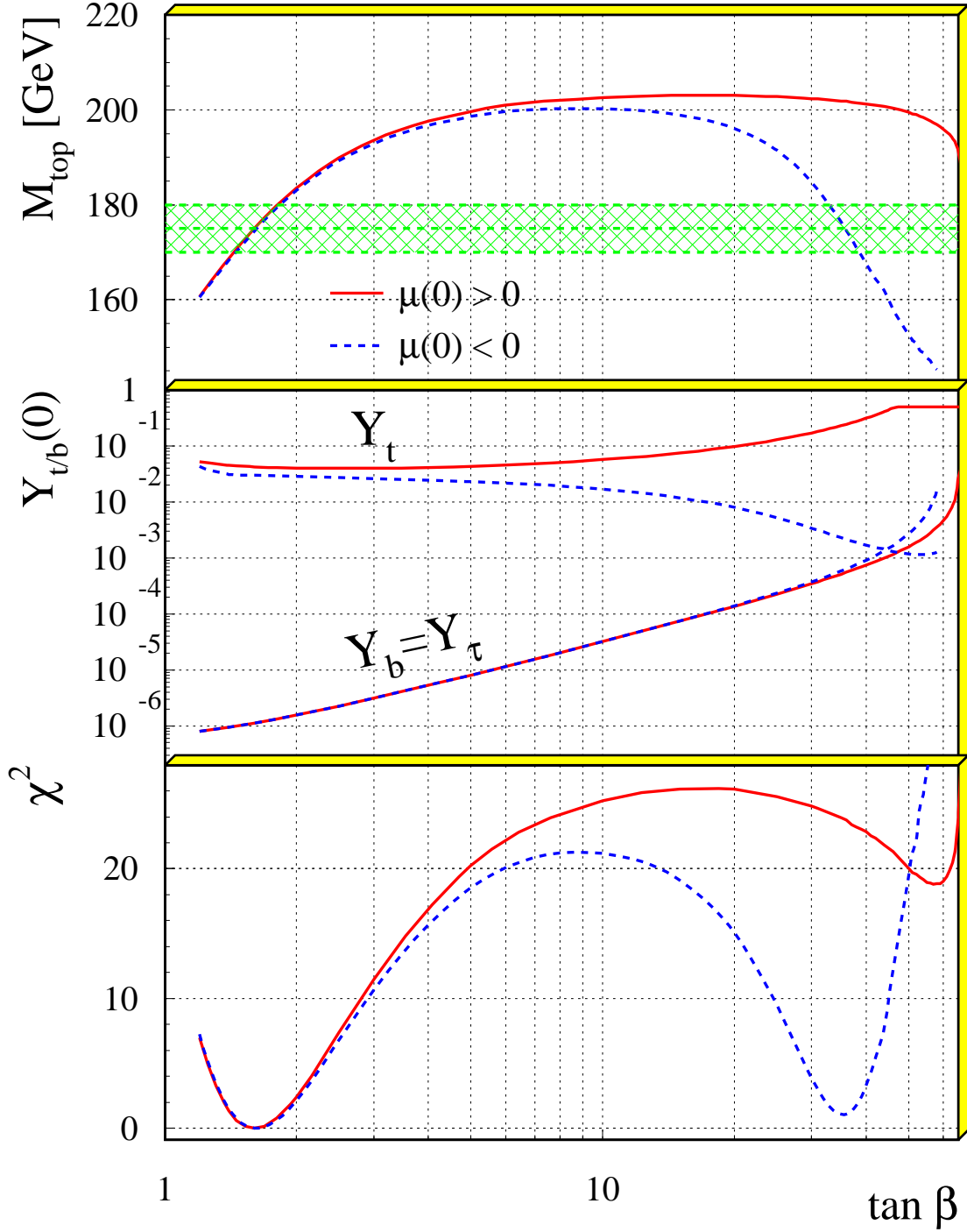


Figure 1: The upper part shows the top quark mass as function of $\tan \beta$ for $m_0 = 600$ GeV, $m_{1/2} = 400$ GeV. The middle part shows the corresponding values of the Yukawa couplings at the GUT scale and the lower part the χ^2 values, which show that the value of $\tan \beta$ are restricted to the following ranges $1 < \tan \beta < 2$ or $30 < \tan \beta < 40$ for $\mu < 0$.

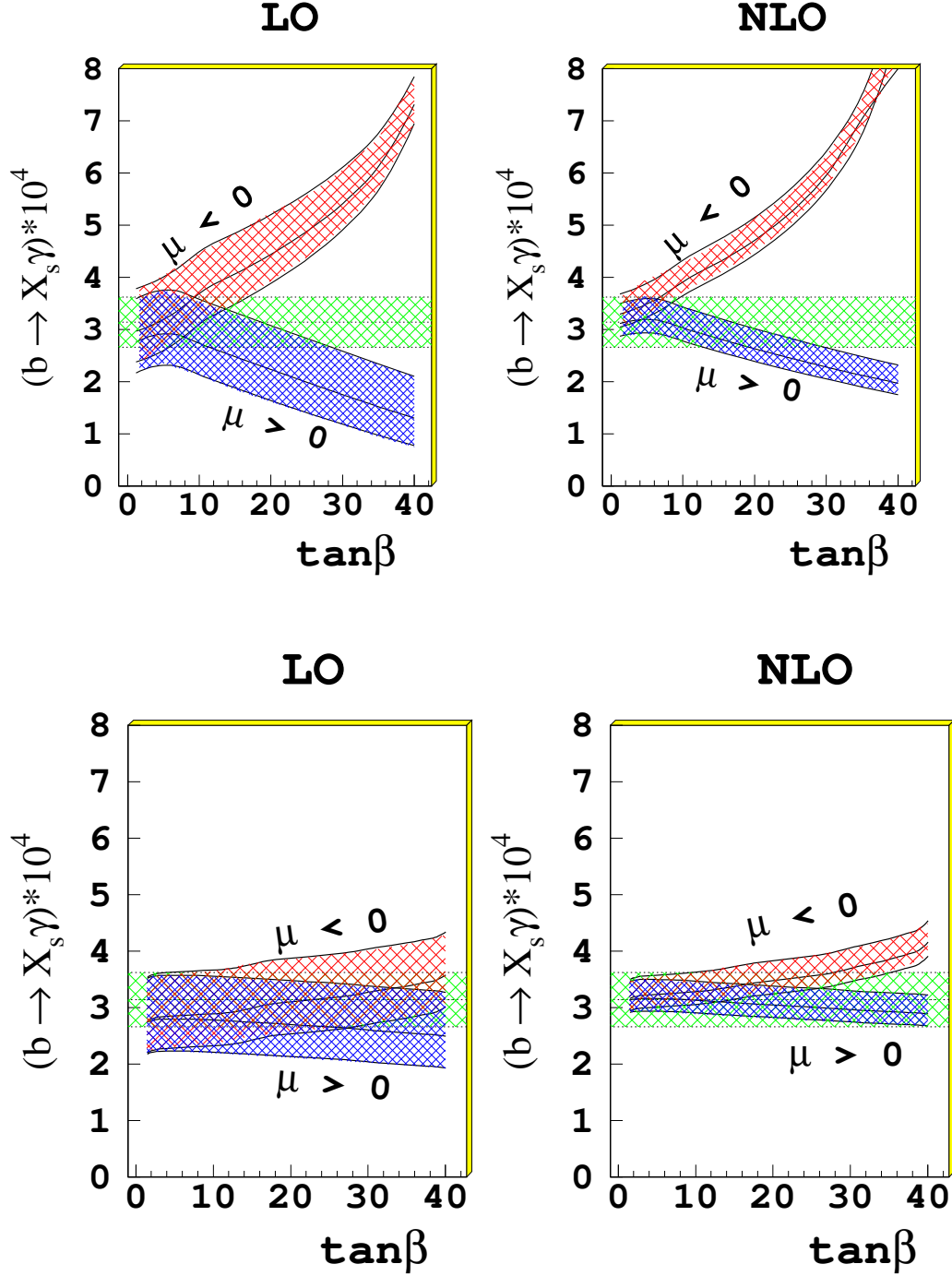


Figure 2: The dependence of the $b \rightarrow X_s \gamma$ rate on $\tan \beta$ for LO (l.h.s.) and NLO (r.h.s.) for $A_0 = 0$ and $m_0 = 600$ (1000) GeV, $m_{1/2} = 400$ (1000) GeV at the top (bottom). For each value of $\tan \beta$ a fit was made to bring the predicted $b \rightarrow X_s \gamma$ rate (curved bands) as close as possible to the data (horizontal bands). The width of the predicted values shows the renormalization scale uncertainty from a scale variation between $0.5m_b$ and $2m_b$. Clearly, good agreement with the data at large $\tan \beta$ is only achieved for heavy sparticles.

$$\tan \beta = 35, \mu < 0$$

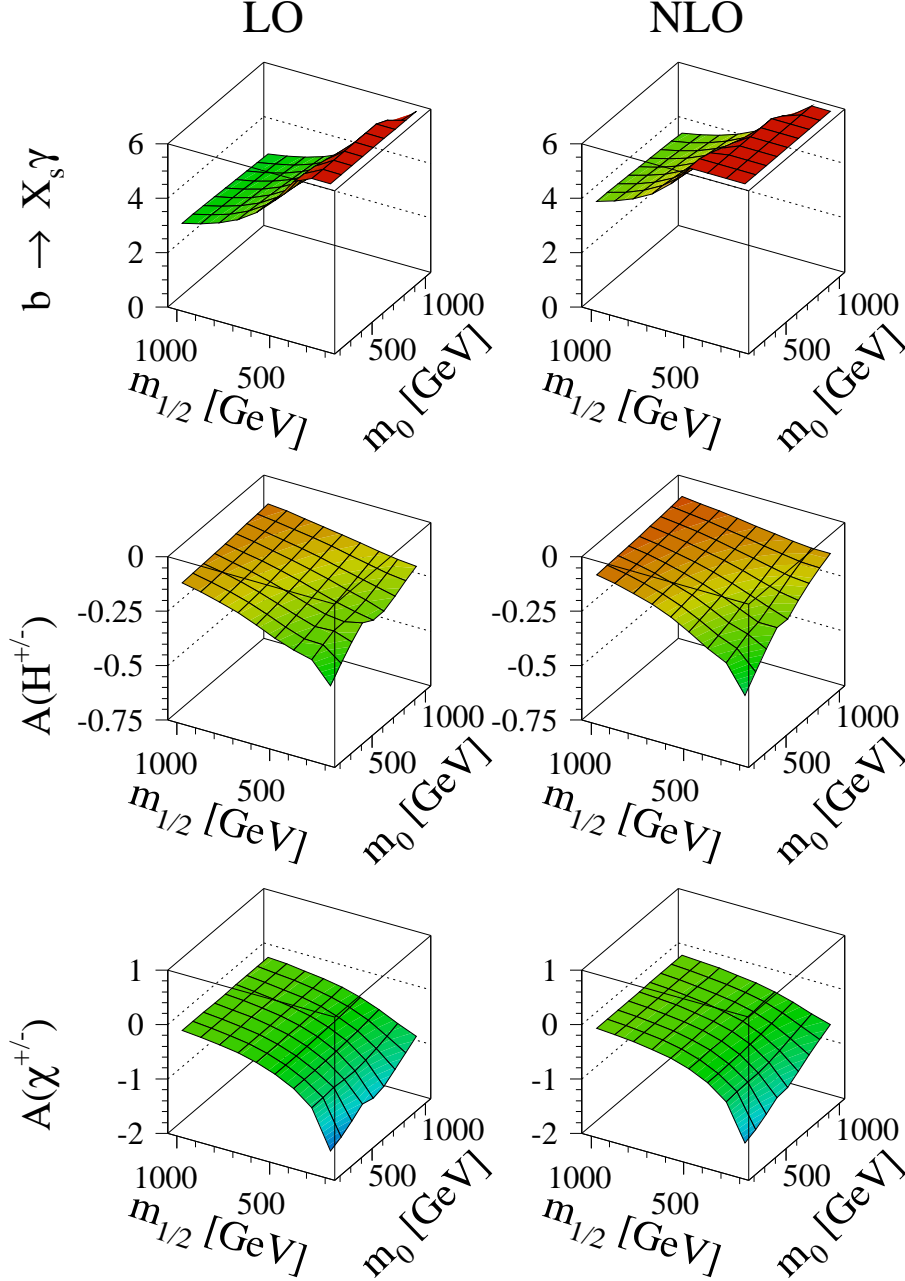


Figure 3: The decay rate (in units of 10^{-4}) and selected amplitudes (in units of 10^{-2}) of the $b \rightarrow X_s \gamma$ decay for negative μ and $\tan \beta = 35$. These amplitudes should be compared with the SM amplitude of $-0.56 \cdot 10^{-2}$.

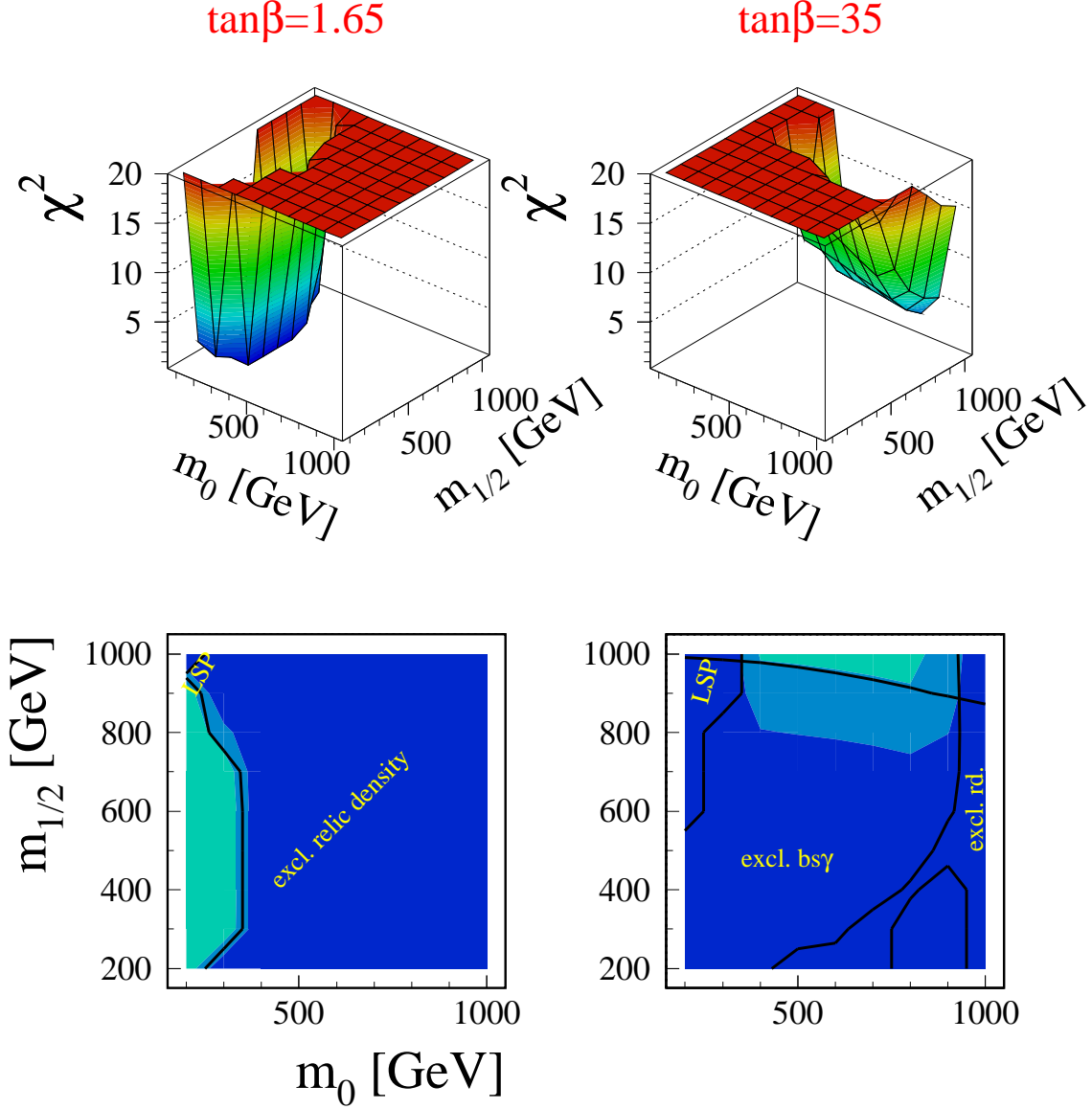


Figure 4: The upper row shows the χ^2 distribution in the m_0 – $m_{1/2}$ plane for $\tan\beta = 1.65$ and $\tan\beta = 35$ with $\mu > 0$ and $\mu < 0$, respectively. The projections are shown in the second row. The different shades in the projections indicate steps of $\Delta\chi^2 = 4$. The contour lines show areas excluded by the particular constraints used in the analysis: in the LSP area the Lightest Supersymmetric Particle is charged (usually the stau), which is not allowed if the LSP is stable, in the relic density (rd) area the density of the universe is above the critical density and in the $bs\gamma$ area the $b \rightarrow X_s\gamma$ rate is too high. The μ_b renormalization scale was allowed to vary between $0.5m_b$ and $2m_b$ for the $b \rightarrow X_s\gamma$ rate.

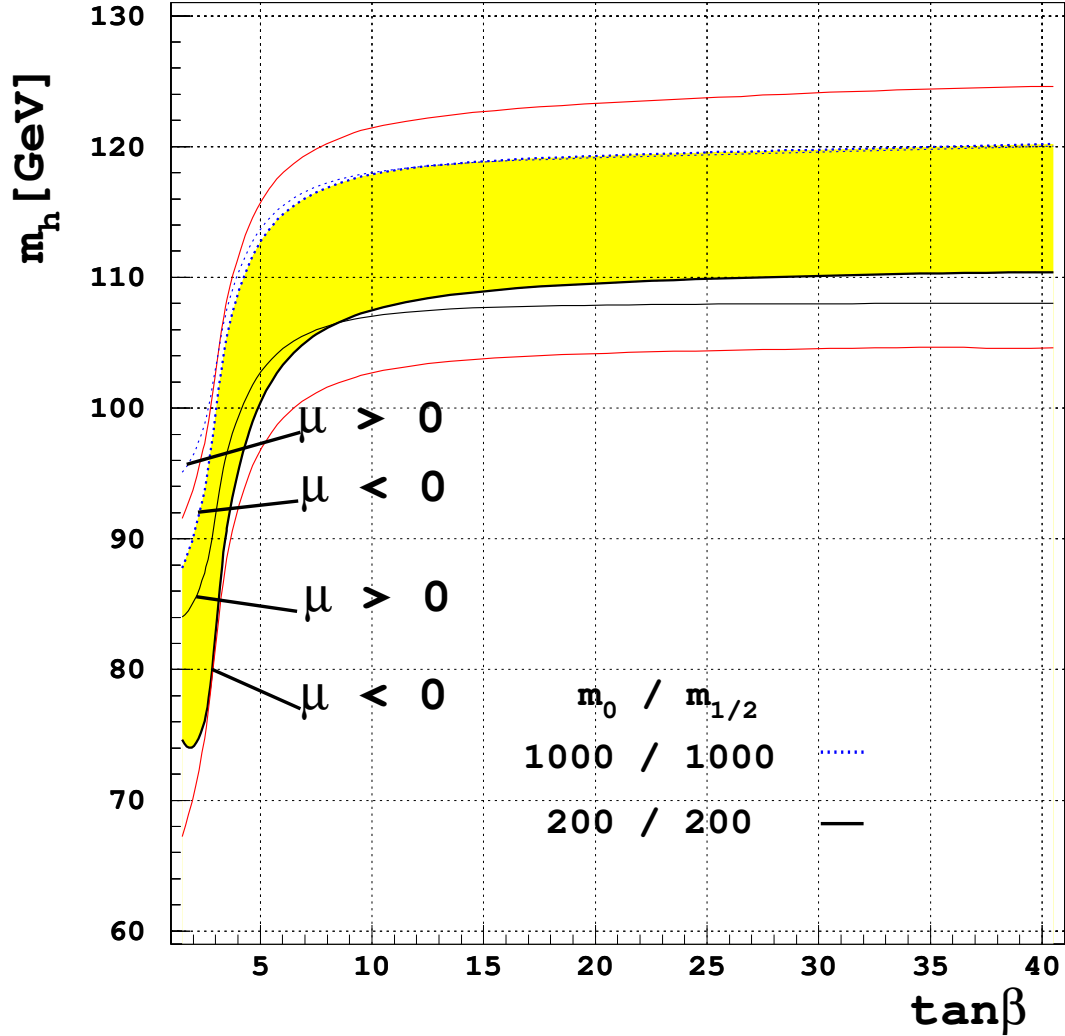


Figure 5: The mass of the lightest Higgs boson as function of $\tan \beta$, as calculated by the effective potential approach[26]. The shaded band shows the variation of $m_0 = m_{1/2}$ between 200 and 1000 GeV for $\mu < 0$, $m_t = 175$ GeV, and $A_0 = 0$. Note the small dependence on the sign of μ for large $\tan \beta$, as expected from the suppression of μ by $\tan \beta$ in the stop mixing. The maximum (minimum) Higgs boson mass value, shown by the upper (lower) line are obtained for $A_0 = -3m_0$, $m_t = 180$ GeV, $m_0 = m_{1/2} = 1000$ GeV ($A_0 = 3m_0$, $m_t = 170$ GeV, $m_0 = m_{1/2} = 200$ GeV). As can be seen the curves show an asymptotic behaviour for large values of $\tan \beta$.

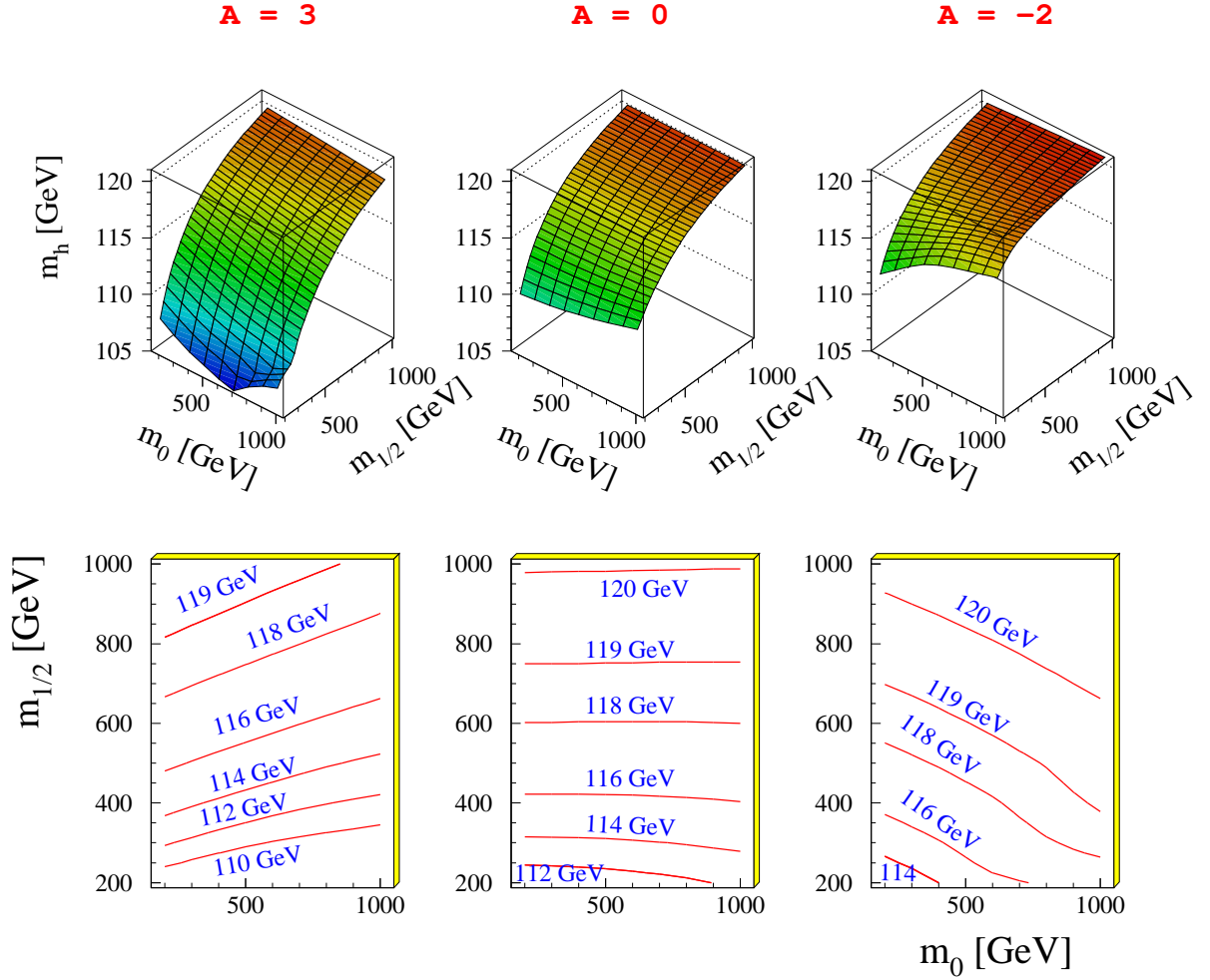


Figure 6: The Higgs boson mass as function of m_0 and $m_{1/2}$, for three values of the trilinear coupling A in units of m_0 as calculated by the effective potential approach[26]. The top mass is 175 GeV and $\tan \beta$ is large, so the results are independent of the precise value of $\tan \beta$. Clearly, for $A = -2m_0$ the excluded area by the present Higgs limit of 113.5 GeV is only the small lefthanded corner.

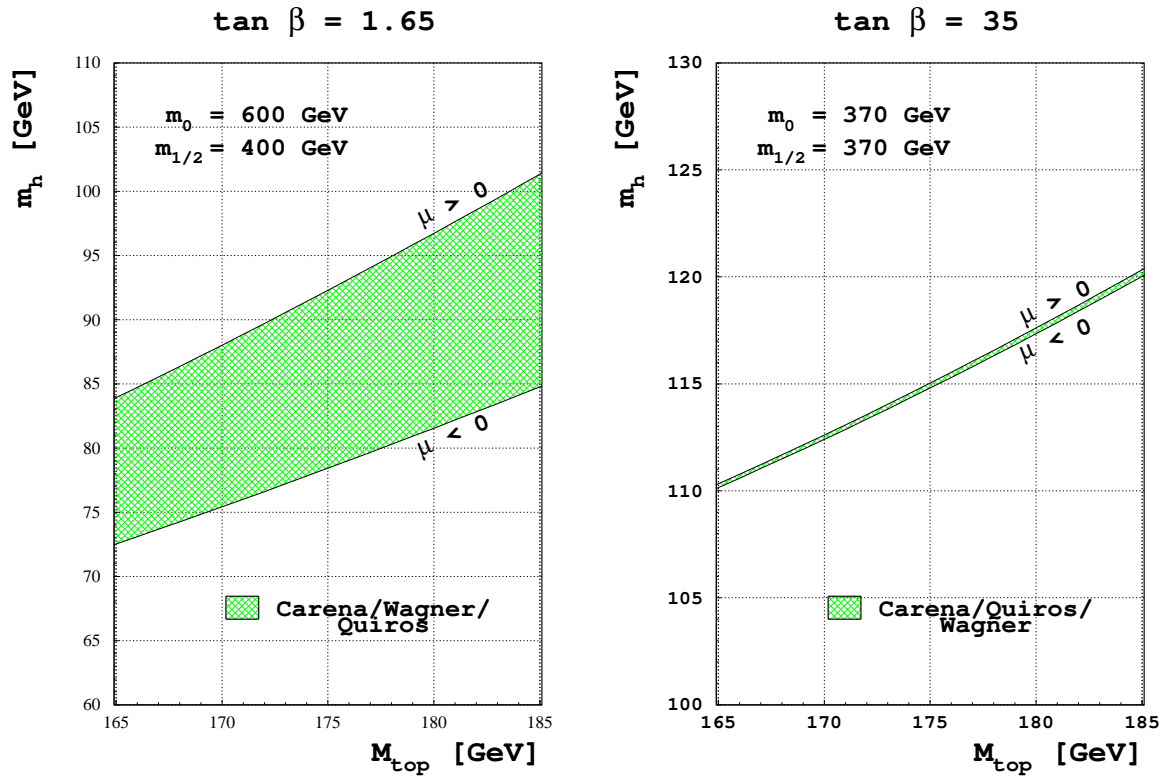


Figure 7: The top mass dependence of the Higgs mass in the low and high $\tan \beta$ scenario. Note the reduced dependence on the sign of μ for large $\tan \beta$.